

# Generalization analysis of an unfolding network for analysis-based Compressed Sensing

Vicky Kouni and Yannis Panagakis

*Department of Informatics & Telecommunications  
National & Kapodistrian University of Athens, Greece  
Email: {vicky-kouni, yannis@di.uoa.gr}*

## Abstract

Unfolding networks have shown promising results in the Compressed Sensing (CS) field. Yet, the investigation of their generalization ability is still in its infancy. In this paper, we perform generalization analysis of a state-of-the-art ADMM-based unfolding network, which jointly learns a decoder for CS and a sparsifying redundant analysis operator. To this end, we first impose a structural constraint on the learnable sparsifier, which parametrizes the network’s hypothesis class. For the latter, we estimate its Rademacher complexity. With this estimate in hand, we deliver generalization error bounds for the examined network. Finally, the validity of our theory is assessed and numerical comparisons to a state-of-the-art unfolding network are made, on synthetic and real-world datasets. Our experimental results demonstrate that our proposed framework complies with our theoretical findings and outperforms the baseline, consistently for all datasets.

**Keywords**— compressed sensing, deep unfolding, unfolding network, analysis sparsity, generalization error bounds, Rademacher complexity

## 1 Introduction

*Compressed Sensing* (CS) is a modern technique for recovering signals  $x \in \mathbb{R}^n$  from incomplete, noisy observations  $y = Ax + e \in \mathbb{R}^{m \times n}$ ,  $m < n$ . To date, various optimization algorithms are employed for tackling the CS problem [1], [2], [3], [4]. However, the fact that model-based methods may lack in terms of time complexity and/or reconstruction quality, has led researchers to develop data-driven approaches for dealing with CS [5], [6], [7]. In a recent line of research, the merits of iterative methods and deep neural networks are combined in *deep unfolding* [8], [9]. The latter constitutes a technique for interpreting the iterations of optimization algorithms as layers of a neural network, which reconstructs the signals of interest from their compressive measurements.

Deep unfolding networks (DUNs) for inverse problems [10], [11] are preferred to standard deep learning architectures, since they enjoy advantages like interpretability [12], prior knowledge of signal structure [13] and a relatively small number of trainable parameters [14]. The same holds true in the case of CS, where state-of-the-art (SotA) unfolding networks [15], [16], [17], [18], [19] typically learn a function called *decoder*, which reconstructs  $x$  from  $y$ . In fact, unfolding networks based on the *iterative soft-thresholding algorithm* (ISTA [2]) and the *alternating direction of multipliers method* (ADMM [4]) seem to be the most popular classes of DUNs targeting the CS problem. Such networks can also learn – jointly with the decoder – a sparsifying transform for the data [20], [21], [22], [23], [24], [25], integrating that way a dictionary learning technique. Due to the advantages that the latter has offered when applied in model-based methods [26], [27], [28], it seems intriguing to examine its effectiveness when combined with DUNs.

Nevertheless, most of the aforementioned ISTA- and ADMM-based DUNs promote synthesis sparsity [29] in their framework, since the learnable sparsifying dictionary satisfies some orthogonality constraint. Distinct from its synthesis counterpart [30], the analysis sparsity model may be more advantageous for CS [31]. For example, it takes into account the redundancy of the involved analysis operators, leading to a more flexible sparse representation of the signals, as opposed to orthogonal sparsifiers [32] (see Section 2 for a detailed comparison between the two sparsity models). To our knowledge, only one SotA ADMM-based DUN [24] – which comprises the preliminary work of this article – solves the CS problem by entailing analysis sparsity, in terms of learning a sparsifying redundant analysis operator.

From the mathematical viewpoint, the generalization analysis of deep neural networks [33], [34] attracts significant research interest [35], [36], [37], [38]. Nevertheless, the estimation the generalization error of DUNs is still at an early stage. Particularly, generalization error bounds are mainly provided for the class of ISTA-based unfolding networks [20], [39], [40]. To our knowledge, the generalization ability of ADMM-based DUNs is not yet explained.

In this paper, distinct from the previous methods, we leverage a “built-in” characteristic of ADMM to impose specific structure on the learnable sparsifying redundant transform of a SotA ADMM-based DUN, namely ADMM-DAD [24]. For the latter, we estimate its generalization error, in terms of the Rademacher complexity of its associated hypothesis class. In the end, we present empirical evidence supporting our derived generalization error bounds. Our contributions are summarized below.

1. Inspired by recent representatives of the classes of ISTA- and ADMM-based unfolding networks [20], [22], [23], [24] (see Section 2 for a brief description of a subset of them), we address the generalization analysis of a SotA ADMM-based DUN, namely ADMM-DAD [24], which deals with analysis-based CS. Towards that direction, we first exploit inherent structure of the original ADMM algorithm and impose a structural constraint on the learnable sparsifier of ADMM-DAD. Our proposed framework – presented in Section 3.1 – induces a frame property in the learnable redundant analysis operator, which parametrizes/“enhances” the hypothesis class of ADMM-DAD. To our knowledge, we are the first to impose such a structure on the hypothesis class of a DUN solving the analysis-based CS problem.
2. In Section 3.4, we employ chaining to estimate the Rademacher complexity of the enhanced hypothesis class of ADMM-DAD. Our novelty lies on studying the generalization ability of this ADMM-based DUN, by means of the afore-stated

Rademacher estimate. The generalization error bounds for ADMM-DAD are presented in Section 3.5.

3. We verify our theoretical guarantees in Section 4, by numerically testing ADMM-DAD on a synthetic dataset and a real-world image dataset, i.e., MNIST [41]. We also compare the performance of ADMM-DAD to that of a recent variant of ISTA-net [20]. In all experiments, ADMM-DAD outperforms the baseline and its generalization ability conforms with our theoretical results.

*Notation.* For a sequence  $a_n$  that is upper bounded by  $M > 0$ , we write  $\{a_n\} \leq M$ . For a matrix  $A \in \mathbb{R}^{m \times n}$ , we write  $\|A\|_{2 \rightarrow 2}$  for its operator/spectral norm and  $\|A\|_F$  for its Frobenius norm. The  $l_2$ -norm of a vector in  $\mathbb{R}^n$  is represented by  $\|\cdot\|_2$ . For a family of vectors  $(\phi_i)_{i=1}^N$  in  $\mathbb{R}^n$ ,  $N > n$ , its associated analysis operator is given by  $\Phi x := \{\langle x, \phi_i \rangle\}_{i=1}^N$ , where  $x \in \mathbb{R}^n$ . The adjoint of  $\Phi$ , i.e.  $\Phi^T$ , is the synthesis operator. Moreover,  $\{\phi_i\}_{i=1}^N$  is a *frame* for  $\mathbb{R}^n$  if it holds

$$\alpha \|x\|_2^2 \leq \sum_{i=1}^N |\langle x, \phi_i \rangle|^2 \leq \beta \|x\|_2^2 \quad (1)$$

for all  $x \in \mathbb{R}^n$ , for some  $0 < \alpha \leq \beta < \infty$  (frame bounds);  $\alpha$  is the *lower frame bound* and  $\beta$  is the *upper frame bound*. We denote with  $S$  the multiplication of a synthesis with an analysis operator, i.e.  $S = \Phi^T \Phi \in \mathbb{R}^{n \times n}$ , and call it *S-operator*. Moreover, if  $S$  is invertible, then  $(\phi_i)_{i=1}^N$  is a frame and we call  $S$  the *frame operator* associated with that frame. For the frame operator and its inverse, it holds  $\alpha \leq \|S\|_{2 \rightarrow 2} \leq \beta$  and  $\beta^{-1} \leq \|S^{-1}\|_{2 \rightarrow 2} \leq \alpha^{-1}$ , respectively. For matrices  $A_1, A_2 \in \mathbb{R}^{N \times n}$ , we denote by  $[A_1; A_2] \in \mathbb{R}^{2N \times n}$  their concatenation with respect to the first dimension, while we denote by  $[A_1 | A_2] \in \mathbb{R}^{N \times 2n}$  their concatenation with respect to the second dimension. We write  $O_{N \times N}$  for a real-valued  $N \times N$  matrix filled with zeros and  $I_{N \times N}$  for the  $N \times N$  identity matrix. For  $x \in \mathbb{R}$ ,  $\tau > 0$ , the soft thresholding operator  $\mathcal{S}_\tau : \mathbb{R} \mapsto \mathbb{R}$  is defined as

$$\mathcal{S}_\tau(x) = \mathcal{S}(x, \tau) = \begin{cases} \text{sign}(x)(|x| - \tau), & |x| \geq \tau \\ 0, & \text{otherwise,} \end{cases} \quad (2)$$

or in closed form  $\mathcal{S}(x, \tau) = \text{sign}(x) \max(0, |x| - \tau)$ . For  $x \in \mathbb{R}^n$ , the soft thresholding operator acts component-wise, i.e.  $(\mathcal{S}_\tau(x))_i = \mathcal{S}_\tau(x_i)$ , and is 1-Lipschitz with respect to  $x$ . For  $y \in \mathbb{R}^n$ ,  $\tau > 0$ , the mapping

$$P_G(\tau; y) = \operatorname{argmin}_{x \in \mathbb{R}^n} \left\{ \tau G(x) + \frac{1}{2} \|x - y\|_2^2 \right\}, \quad (3)$$

is the *proximal mapping associated to the convex function*  $G$ . For  $G(\cdot) = \|\cdot\|_1$ , (3) coincides with (2). For two functions  $f, g : \mathbb{R}^n \mapsto \mathbb{R}^n$ , we write their composition as  $f \circ g : \mathbb{R}^n \mapsto \mathbb{R}^n$  and if there exists some constant  $C > 0$  such that  $f(x) \leq Cg(x)$ , then we write  $f(x) \lesssim g(x)$ . For the ball of radius  $t > 0$  in  $\mathbb{R}^n$  with respect to some norm  $\|\cdot\|$ , we write  $B_{\|\cdot\|}^n(t)$ . The covering number  $\mathcal{N}(T, \|\cdot\|, t)$  of a space  $T$ , equipped with a norm  $\|\cdot\|$ , at level  $t > 0$ , is defined as the smallest number of balls  $B_{\|\cdot\|}^n(t)$ , required to cover  $T$ .

## 2 Background on sparsity models and unfolding networks for CS

### 2.1 Synthesis-based CS: unfolding ISTA and ADMM

CS aims at recovering  $x \in \mathbb{R}^n$  from  $y = Ax + e \in \mathbb{R}^m$ ,  $m < n$ , with  $A$  being the measurement matrix and  $e \in \mathbb{R}^m$ ,  $\|e\|_2 \leq \epsilon$ , corresponding to noise. To do so, one can impose a synthesis sparsity model on  $x$  [29], [42], i.e., assume that there exists  $D \in \mathbb{R}^{n \times p}$  ( $n \leq p$ ) such that  $x = Dz$ , with the coefficients' vector  $z \in \mathbb{R}^p$  being sparse. In fact,  $D$  is typically chosen to be an orthogonal matrix, e.g. a wavelet or cosine transform. By incorporating synthesis sparsity in CS, one is called to solve the LASSO problem:

$$\min_{z \in \mathbb{R}^n} \frac{1}{2} \|y - \tilde{A}z\|_2^2 + \lambda \|z\|_1, \quad (4)$$

with  $\tilde{A} = AD$  and  $\lambda > 0$  being a regularization parameter. Two broad classes of algorithms that are commonly employed to solve (4) rely on ISTA and ADMM. These methods incorporate a proximal mapping (3) and yield iterative schemes which, under mild assumptions, output a minimizer  $\hat{z}$  of (4); then the desired reconstructed signal is simply given by  $\hat{x} = D\hat{z}$ . If  $D$  is regarded unknown and learned from a sequence of training samples, the iterations of ISTA and ADMM are interpreted as layers of neural networks; such DUNs are usually coined ISTA-nets [20], [43] and ADMM-nets [22, 44], respectively. They jointly learn sparsifying transforms for the data and a decoder for CS, that is, a function reconstructing  $x$  from  $y$ .

### 2.2 Analysis-based CS: unfolding ADMM

The algorithms and corresponding DUNs we described so far rely on the synthesis sparsity model, since their framework incorporates some orthogonality constraint for the learnable sparsifiers. A tractable counterpart of synthesis sparsity is the analysis sparsity model [45], [46], [32], (also known as cosparsity model [30], [47]). In the latter, one assumes that there exists some *redundant analysis operator*  $\Phi \in \mathbb{R}^{N \times n}$ ,  $N > n$ , such that  $\Phi x$  is sparse. Under the analysis sparsity model, the optimization problem for CS is formulated as a generalized LASSO problem, i.e.,

$$\min_{x \in \mathbb{R}^n} \frac{1}{2} \|Ax - y\|_2^2 + \lambda \|\Phi x\|_1. \quad (5)$$

Particularly, analysis sparsity has gained research interest, due to some advantages it may offer compared to its synthesis counterpart. For example, the redundancy of an analysis operator associated to a frame [48] can provide greater – than orthonormal bases – flexibility in the sparse representation of signals [49]. Moreover, it is computationally more efficient to use sparsifying redundant transforms instead of orthogonal ones, since the iterative algorithm for CS may need less measurements  $m$  for perfect reconstruction [32]. Especially when  $D \in \mathbb{R}^{n \times p}$ ,  $n < p$ , so that the optimization variable in (4) lies in  $\mathbb{R}^p$ , one can argue that it is preferable to solve (5), since the dimension of the optimization problem is smaller [31]. Now, thresholding algorithms like ISTA cannot treat analysis sparsity, since the proximal mapping associated to  $\|\Phi(\cdot)\|_1$  does not have a closed-form solution. Therefore, we turn to ADMM, which can efficiently

solve (5) by means of the following iterative scheme:

$$x^{k+1} = (A^T A + \rho \Phi^T \Phi)^{-1} (A^T y + \rho \Phi^T (z^k - u^k)) \quad (6)$$

$$z^{k+1} = \mathcal{S}_{\lambda/\rho}(\Phi x^{k+1} - u^k) \quad (7)$$

$$u^{k+1} = u^k + \Phi x^{k+1} - z^{k+1}, \quad (8)$$

$z, u \in \mathbb{R}^N$ . Let us suppose that the redundant analysis operator  $\Phi$  is unknown and learned from a set of i.i.d. training samples, i.e.  $\mathbf{S} = \{(x_i, y_i)\}_{i=1}^s$ , drawn from an unknown distribution<sup>1</sup>  $\mathcal{D}^s$ . Then, the updates in (6) - (8) can be interpreted as a neural network with  $L \in \mathbb{N}$  layers, coined ADMM Deep Analysis Decoding (ADMM-DAD) [24]. The output of the first and the  $k$ th layer are given by

$$f_1(y) = I' b(y) + I'' \mathcal{S}_{\lambda/\rho}(b(y)), \quad (9)$$

$$f_k(v) = \tilde{\Theta} v + I' b + I'' \mathcal{S}_{\lambda/\rho}(\Theta v + b), \quad k = 2, \dots, L, \quad (10)$$

respectively, with  $R = A^T A + \rho \Phi^T \Phi \in \mathbb{R}^{n \times n}$ ,  $W = \rho \Phi R^{-1} \Phi^T \in \mathbb{R}^{N \times N}$ ,  $b = b(y) = \Phi R^{-1} A^T y \in \mathbb{R}^{N \times 1}$ ,  $\Lambda = (I - W | W) \in \mathbb{R}^{N \times 2N}$ ,  $\Theta = (-I - W | W) \in \mathbb{R}^{N \times 2N}$ ,  $\tilde{\Theta} = [\Lambda; O_{N \times 2N}] \in \mathbb{R}^{2N \times 2N}$ ,  $I_1 = [I_{N \times N}; O_{N \times N}] \in \mathbb{R}^{2N \times N}$ ,  $I_2 = [-I_{N \times N}; I_{N \times N}] \in \mathbb{R}^{2N \times N}$ . For more details on the unrolling procedure, we refer the interested reader to [24].

The composition of  $L$  such layers (all having the same  $\Phi$ ) is denoted by

$$f_{\Phi}^L(y) = f_L \circ \dots \circ f_1(y) \quad (11)$$

and constitutes an *intermediate decoder* – realized by ADMM-DAD – that reconstructs the *intermediate variable*  $v$  from  $y$ . Motivated by (6), we acquire the desired solution  $\hat{x}$  by applying an affine map  $T : \mathbb{R}^{2N \times 1} \mapsto \mathbb{R}^{n \times 1} : v \mapsto Cv + \tau$  after the final layer  $L$ , so that

$$\hat{x} := Cv + \tau, \quad (12)$$

where

$$C = [-\rho R^{-1} \Phi^T | \rho R^{-1} \Phi^T] \in \mathbb{R}^{n \times 2N}, \quad (13)$$

$$\tau = R^{-1} A^T y \in \mathbb{R}^n, \quad (14)$$

with  $[u^L; z^L] = v_L$ . Finally, the application of an appropriate clipping function

$$\sigma(x) = \begin{cases} x, & \|x\|_2 \leq B_{\text{out}} \\ B_{\text{out}} \frac{x}{\|x\|_2}, & \text{otherwise} \end{cases}, \quad (15)$$

for some fixed constant  $B_{\text{out}} > 0$ , so that the output is pushed inside a reasonable range of values, yields the desired decoder, i.e.,

$$\text{dec}_{\Phi}^L(y) = \sigma(T(f_{\Phi}^L(y))), \quad (16)$$

implemented by ADMM-DAD.

---

<sup>1</sup>Formally speaking, this is a distribution over  $x_i$  and for fixed  $A, e$ , we obtain  $y_i = Ax_i + e$

### 3 Generalization Analysis of ADMM-DAD

#### 3.1 Enhancing the hypothesis class of ADMM-DAD

According to [24], the hypothesis class of ADMM-DAD consists of all the decoders that ADMM-DAD can implement and is parametrized by the learnable redundant analysis operator  $\Phi$ :

$$\mathcal{H}^L = \{\sigma \circ h : \mathbb{R}^m \mapsto \mathbb{R}^n : h(y) = T(f_\Phi^L(y)), \Phi \in \mathbb{R}^{N \times n}, N > n\}. \quad (17)$$

However, the definition of (17) does not account for any particular structure on  $\Phi$ , which in turn could explain the performance of ADMM-DAD. On the other hand, the  $x$ -update (6) of ADMM incorporates the term  $S = \Phi^T \Phi$ , which is typically assumed to be an invertible matrix [4], [50]. Similarly, typical choices for the measurement matrix  $A$  consist of a (appropriately normalized) Gaussian matrix [29], [51], [52]. Therefore, we are inspired by the aforementioned facts and make some assumptions, which will hold for the rest of the paper.

**Assumption 3.1.** *For an analysis operator  $\Phi \in \mathbb{R}^{N \times n}$  with  $N > n$ , the matrix  $S = \Phi^T \Phi$  is invertible.*

**Assumption 3.2.** *For an analysis operator satisfying Assumption 3.1, and for appropriately chosen measurement matrix  $A \in \mathbb{R}^{m \times n}$  and penalty parameter  $\rho > 0$ , it holds  $\rho \|S^{-1}\|_{2 \rightarrow 2} \|A\|_{2 \rightarrow 2} < 1$ .*

**Remark 3.1.** *From a theoretical perspective, it is reasonable to incorporate the invertibility of  $S$  in our framework, since the set of non-invertible matrices  $S$  of the form  $S = \Phi^T \Phi$  has zero Lebesgue measure. Additionally, Assumptions 3.1 and 3.2 are empirically confirmed (see Section 4.1.4), since ADMM-DAD learns a  $\Phi$  with associated  $S$ -operator satisfying  $S^{-1}S = I$  and  $\rho \|S^{-1}\|_{2 \rightarrow 2} \|A\|_{2 \rightarrow 2} < 1$ .*

Due to Assumption 3.1, we can further assume that there exists some  $0 < \beta < \infty$ , so that  $\|S\|_{2 \rightarrow 2} \leq \beta$ , which leads us to introduce the following definition.

**Definition 3.2.** *We define  $\mathcal{F}_\beta$  to be the class of redundant analysis operators  $\Phi \in \mathbb{R}^{N \times n}$  for which the associated  $S$ -operator is invertible and has bounded operator norm by some  $0 < \beta < \infty$ .*

**Remark 3.3.** *The invertibility of  $S$  in Definition 3.2 implies that the rows of  $\Phi$  constitute a frame for  $\mathbb{R}^n$ . Hence,  $S$  is a frame operator and for some  $0 < \alpha \leq \beta < \infty$ , it holds  $\alpha \leq \|S\|_{2 \rightarrow 2} \leq \beta$  and  $\|\Phi\|_{2 \rightarrow 2} \leq \sqrt{\beta}$ .*

We enhance the hypothesis class of ADMM-DAD with the framework we described so far, in order to account for a structural constraint on  $\Phi$ .

**Definition 3.4.** *The enhanced hypothesis class  $\mathbf{H}^L$  of ADMM-DAD is parameterized by  $\Phi \in \mathcal{F}_\beta$  and is defined as the space of all the decoders that ADMM-DAD can implement, i.e.,*

$$\mathbf{H}^L = \{h : \mathbb{R}^m \mapsto \mathbb{R}^n : h(y) = \sigma(T(f_\Phi^L(y))), \Phi \in \mathcal{F}_\beta\}. \quad (18)$$

Given the hypothesis class (18) and the training set  $\mathbf{S}$ , ADMM-DAD yields  $h \in \mathbf{H}^L$  such that  $h(y) = \hat{x} \approx x$ . For a loss function  $\ell : \mathbf{H}^L \times \mathbb{R}^n \times \mathbb{R}^m \mapsto \mathbb{R}_{>0}$ , we define the empirical loss of a hypothesis  $h \in \mathbf{H}^L$  as

$$\hat{\mathcal{L}}_{train}(h) = \frac{1}{s} \sum_{i=1}^s \ell(h, x_i, y_i). \quad (19)$$

For the rest of the paper, we work with  $\ell(\cdot) = \|\cdot\|_2^2$ , so that (19) transforms into the *training mean-squared error* (train MSE):

$$\hat{\mathcal{L}}_{train}(h) = \frac{1}{s} \sum_{j=1}^s \|h(y_j) - x_j\|_2^2. \quad (20)$$

We also define the *true loss* to be

$$\mathcal{L}(h) = \mathbb{E}_{(x,y) \sim \mathcal{D}} (\|h(y) - x\|_2^2). \quad (21)$$

The difference between (20) and (21), i.e.,

$$\text{GE}(h) = |\hat{\mathcal{L}}_{train}(h) - \mathcal{L}(h)|, \quad (22)$$

constitutes the *generalization error* of ADMM-DAD and informs us about how well the network performs on unseen data. Since  $\mathcal{D}$  is unknown, we estimate (22) in terms of the *empirical Rademacher complexity* [33]:

$$\mathcal{R}_{\mathbf{S}}(\ell \circ \mathbf{H}^L) = \mathbb{E} \sup_{h \in \mathbf{H}^L} \frac{1}{s} \sum_{i=1}^s \epsilon_i \|h(y_i) - x_i\|_2^2, \quad (23)$$

with  $\epsilon$  being a Rademacher vector, i.e, a vector with i.i.d. entries taking the values  $\pm 1$  with equal probability. The following Theorem provides exactly what we need.

**Theorem 3.5** ([33, Theorem 26.5]). *Let  $\mathcal{H}$  be a family of functions,  $\mathcal{S}$  the training set drawn from  $\mathcal{D}^s$ , and  $\ell$  a real-valued bounded loss function satisfying  $|\ell(h, z)| \leq c$ , for all  $h \in \mathcal{H}, z \in Z$ . Then, for  $\delta \in (0, 1)$ , with probability at least  $1 - \delta$ , we have for all  $h \in \mathcal{H}$*

$$\mathcal{L}(h) \leq \hat{\mathcal{L}}_{train}(h) + 2\mathcal{R}_{\mathcal{S}}(\ell \circ \mathcal{H}) + 4c \sqrt{\frac{2 \log(4\delta)}{s}}. \quad (24)$$

In order to apply the latter in  $\mathbf{H}^L$ , we prove that  $\|\cdot\|_2^2$  is bounded by some constant  $c > 0$ . Towards that direction, we make two typical – for the machine learning literature – assumptions for  $\mathbf{S}$ . Let us suppose that with overwhelming probability it holds:

$$\|y_i\|_2 \leq B_{in}, \quad (25)$$

for some constant  $B_{in} > 0$ ,  $i = 1, 2, \dots, s$ . We also assume that for any  $h \in \mathbf{H}^L$ , with overwhelming probability over  $y_i$  chosen from  $\mathcal{D}$ , it holds

$$\|h(y_i)\|_2 \leq B_{out}, \quad (26)$$

by definition of  $\sigma$ , for some constant  $B_{out} > 0$ ,  $i = 1, 2, \dots, s$ . Then, we have  $\|h(y_i) - x_i\|_2^2 \leq (B_{in} + B_{out})^2$ , for all  $i = 1, 2, \dots, s$ . Hence,  $c = (B_{in} + B_{out})^2$ .

We also simplify the quantity  $\mathcal{R}_{\mathbf{S}}(\|\cdot\|_2^2 \circ \mathbf{H}^L)$ , by using the (vector-valued) contraction principle:

**Lemma 3.6** ([53, Corollary 4]). *Let  $\mathcal{H}$  be a set of functions  $h : \mathcal{X} \mapsto \mathbb{R}^n$ ,  $f : \mathbb{R}^n \mapsto \mathbb{R}^n$  a  $K$ -Lipschitz function and  $\mathcal{S} = \{x_i\}_{i=1}^s$ . Then*

$$\mathbb{E} \sup_{h \in \mathcal{H}} \sum_{i=1}^s \epsilon_i f \circ h(x_i) \leq \sqrt{2}K \mathbb{E} \sup_{h \in \mathcal{H}} \sum_{i=1}^s \sum_{k=1}^n \epsilon_{ik} h_k(x_i), \quad (27)$$

where  $(\epsilon_i)$  and  $(\epsilon_{ik})$  are Rademacher sequences.

The latter allows us to study  $\mathcal{R}_S(\mathbf{H})$  alone. Since it is easy to check that  $\|\cdot\|_2^2$  is Lipschitz continuous, with Lipschitz constant  $\text{Lip}_{\|\cdot\|_2^2} = 2B_{\text{in}} + 2B_{\text{out}}$ , we employ Lemma 3.6 to obtain:

$$\begin{aligned}\mathcal{R}_S(l \circ \mathbf{H}^L) &\leq \sqrt{2}(2B_{\text{in}} + 2B_{\text{out}}) \mathbb{E} \sup_{h \in \mathbf{H}^L} \sum_{i=1}^s \sum_{k=1}^n \epsilon_{ik} h_k(x_i) \\ &= \sqrt{2}(2B_{\text{in}} + 2B_{\text{out}}) \mathcal{R}_S(\mathbf{H}).\end{aligned}\tag{28}$$

Therefore, we are left with estimating (28). We do so in a series of steps, presented in the next subsections.

### 3.2 Bounded outputs

We pass to matrix notation by accounting for the number of samples in the training set  $\mathbf{S}$ . Hence, we apply the Cauchy-Schwartz inequality in (25), (26) yielding

$$\|Y\|_F \leq \sqrt{s}B_{\text{in}},\tag{29}$$

$$\|h(Y)\|_F = \|\psi(\phi(f_\Phi^L(Y)))\|_F \leq \sqrt{s}B_{\text{out}},\tag{30}$$

respectively. We also state below two results that will be needed in some of the proofs later on.

**Lemma 3.7** (Proof in the supplementary material). *Let  $A \in \mathbb{R}^{n \times n}$  be invertible and  $B \in \mathbb{R}^{n \times n}$ . For some norm  $\|\cdot\|$  in  $\mathbb{R}^n$ , if it holds  $\|A^{-1}\| \|B\| < 1$ , then  $A + B \in \mathbb{R}^{n \times n}$  is invertible. Moreover, we have*

$$\|(A + B)^{-1}\| \leq \frac{\|A^{-1}\|}{1 - \|A^{-1}\| \|B\|}.\tag{31}$$

**Lemma 3.8** (Proof in the supplementary material). *For some norm  $\|\cdot\|$  in  $\mathbb{R}^n$ , if  $A, B \in \mathbb{R}^{n \times n}$  are invertible, then*

$$\|B^{-1} - A^{-1}\| \leq \|B^{-1}\| \|A^{-1}\| \|A - B\|.\tag{32}$$

We prove that the output of the intermediate decoder (11) is bounded with respect to the Frobenius norm, after any number of layers  $k < L$ .

**Proposition 3.9.** *Let  $k \in \mathbb{N}$ . For any  $\Phi \in \mathcal{F}_\beta$  and arbitrary  $\lambda, \rho > 0$  in the definition of  $f_\Phi^k$ , we have*

$$\|f_\Phi^k(Y)\|_F \leq 3\|A\|_{2 \rightarrow 2} \|Y\|_F q \sqrt{\beta} \sum_{i=0}^{k-1} 3^i (1 + 2q\rho\beta)^i,\tag{33}$$

where  $q = \frac{\rho}{\alpha - \rho\|A^T A\|_{2 \rightarrow 2}}$ , and  $\alpha$  and  $\beta$  are defined as in Remark 3.3.

*Proof.* We prove (33) via induction. For  $k = 1$ :

$$\|f_\Phi^1(Y)\|_F \leq 3\|B\|_F \leq 3\|A\|_{2 \rightarrow 2} \|Y\|_F \sqrt{\beta} \|(A^T A + \rho\Phi^T \Phi)^{-1}\|_{2 \rightarrow 2},\tag{34}$$

which holds by definition of (9). The invertibility of  $S = \Phi^T \Phi$ , along with Assumption 3.2, Remark 3.3 and Lemma 3.7, imply that

$$\begin{aligned}\|(A^T A + \rho\Phi^T \Phi)^{-1}\|_{2 \rightarrow 2} &= \|(A^T A + \rho S)^{-1}\|_{2 \rightarrow 2} \leq \frac{\rho\|S^{-1}\|_{2 \rightarrow 2}}{1 - \rho\|S^{-1}\|_{2 \rightarrow 2} \|A^T A\|_{2 \rightarrow 2}} \\ &= \frac{\rho}{\alpha - \rho\|A^T A\|_{2 \rightarrow 2}} := q,\end{aligned}\tag{35}$$



where in the last step we used the fact that  $\beta^{-1} \leq \|S^{-1}\|_{2 \rightarrow 2} \leq \alpha^{-1}$ , for some  $0 < \alpha \leq \beta < \infty$ . Substituting (35) into (34) yields  $\|f_\Phi^1(Y)\|_F \leq 3\|A\|_{2 \rightarrow 2}\|Y\|_F q\sqrt{\beta}$ . Suppose now that (33) holds for some  $k \in \mathbb{N}$ . Then, for  $k+1$ :

$$\begin{aligned}
\|f_\Phi^{k+1}(Y)\|_F &\leq \|\tilde{\Theta}\|_{2 \rightarrow 2}\|f_\Phi^k(Y)\|_F + 2\|\Theta\|_{2 \rightarrow 2}\|f_\Phi^k(Y)\|_F + 3\|B\|_F \\
&\leq 3\left((1 + 2\|W\|_{2 \rightarrow 2})\|f_\Phi^k(Y)\|_F + \|B\|_F\right) \\
&\leq 3\left((1 + 2q\rho\beta)\left(3\|A\|_{2 \rightarrow 2}\|Y\|_F q\sqrt{\beta} \sum_{i=0}^{k-1} 3^i(1 + 2q\rho\beta)^i\right)\right. \\
&\quad \left.+ \|A\|_{2 \rightarrow 2}\|Y\|_F q\sqrt{\beta}\right) \\
&= 3\|A\|_{2 \rightarrow 2}\|Y\|_F q\sqrt{\beta} \sum_{i=0}^k 3^i(1 + 2q\rho\beta)^i.
\end{aligned}$$

The proof follows.  $\square$

### 3.3 Lipschitzness with respect to $\Phi$

With the previous result in hand, we prove that the intermediate decoder (11) and the final decoder (16) are Lipschitz continuous with respect to  $\Phi$ .

**Theorem 3.10** (Proof in the supplemental material). *Let  $f_W^L$  defined as in (11),  $L \geq 2$ , and analysis operator  $\Phi \in \mathcal{F}_\beta$ . Then, for any  $\Phi_1, \Phi_2 \in \mathcal{F}_\beta$ , it holds*

$$\|f_{\Phi_1}^L(Y) - f_{\Phi_2}^L(Y)\|_F \leq K_L \|\Phi_1 - \Phi_2\|_{2 \rightarrow 2}, \quad (36)$$

where

$$K_L = qG^L + \sum_{k=2}^L \left( G^{L-k} \left[ qG + 36\beta q^2 \rho(1 + \beta q\rho) \|A\|_{2 \rightarrow 2} \|Y\|_F \sum_{i=0}^{k-2} G^i \right] \right), \quad (37)$$

with  $G = 3(1 + 2\beta q\rho)$ , and  $q, \beta$  as in Proposition 3.9.

**Corollary 3.11.** *Let  $h \in \mathbf{H}^L$  defined as in (18),  $L \geq 2$ , and analysis operator  $\Phi \in \mathcal{F}_\beta$ . Then, for any  $\Phi_1, \Phi_2 \in \mathcal{F}_\beta$ , we have:*

$$\|\sigma(T_1(f_{\Phi_1}^L(Y))) - \sigma(T_2(f_{\Phi_2}^L(Y)))\|_F \leq \Sigma_L \|\Phi_2 - \Phi_1\|_{2 \rightarrow 2}, \quad (38)$$

where

$$\Sigma_L = 2q\rho\sqrt{\beta} \left( K_L + 3\|A\|_{2 \rightarrow 2}\|Y\|_F q(1 + 2\beta q\rho) \sum_{k=0}^{L-1} 3^k(1 + 2\beta q\rho)^k \right), \quad (39)$$

with  $q, \beta$  as in Proposition 3.9 and  $K_L$  as in Theorem 3.10.

*Proof.* By definition,  $\sigma$  is a 1-Lipschitz function. The affine map  $T$  is also Lipschitz continuous, with Lipschitz constant satisfying

$$\text{Lip}_T = \|T\|_{2 \rightarrow 2} \leq 2q\rho\sqrt{\beta}, \quad (40)$$

due to the explicit forms of (13) and (14), with  $q$  and  $\beta$  as in Proposition 3.9. Putting everything together and applying Theorem 3.10 yields

$$\begin{aligned}
& \|\sigma(T_1(f_{\Phi_1}^L(Y))) - \sigma(T_2(f_{\Phi_2}^L(Y)))\|_F \\
& \leq \|T_1(f_{\Phi_1}^L(Y)) - T_2(f_{\Phi_2}^L(Y))\|_F \\
& = \|T_1(f_{\Phi_1}^L(Y)) - T_1(f_{\Phi_2}^L(Y)) + T_1(f_{\Phi_2}^L(Y)) - T_2(f_{\Phi_2}^L(Y))\|_F \\
& \leq \|T_1\|_{2 \rightarrow 2} \|f_{\Phi_2}^L(Y) - f_{\Phi_1}^L(Y)\|_F + \|T_2 - T_1\|_{2 \rightarrow 2} \|f_{\Phi_2}^L(Y)\|_F \\
& \leq 2q\rho\sqrt{\beta}K_L\|\Phi_2 - \Phi_1\|_{2 \rightarrow 2} + \left(3\|A\|_{2 \rightarrow 2}\|Y\|_F q\sqrt{\beta} \sum_{k=0}^{L-1} G^k\right) \|T_2 - T_1\|_{2 \rightarrow 2},
\end{aligned}$$

where  $G = 3(1 + 2q\rho\beta)$ . The introduction of mixed terms and the application of Lemma 3.8 give:

$$\begin{aligned}
& \|T_2 - T_1\|_{2 \rightarrow 2} \\
& \leq 2\rho\|(A^T A + \rho\Phi_2^T \Phi_2)^{-1} \Phi_2^T - (A^T A + \rho\Phi_1^T \Phi_1)^{-1} \Phi_1^T\|_{2 \rightarrow 2} \\
& = 2\rho\|(A^T A + \rho\Phi_2^T \Phi_2)^{-1} \Phi_2^T - (A^T A + \rho\Phi_2^T \Phi_2)^{-1} \Phi_1^T \\
& \quad + (A^T A + \rho\Phi_2^T \Phi_2)^{-1} \Phi_1^T - (A^T A + \rho\Phi_1^T \Phi_1)^{-1} \Phi_1^T\|_{2 \rightarrow 2} \\
& \leq 2\rho\left(q\|\Phi_2 - \Phi_1\|_{2 \rightarrow 2} + \sqrt{\beta}\|(A^T A + \rho\Phi_2^T \Phi_2)^{-1} - (A^T A + \rho\Phi_1^T \Phi_1)^{-1}\|_{2 \rightarrow 2}\right) \\
& \leq 2\rho\left(q\|\Phi_2 - \Phi_1\|_{2 \rightarrow 2} + 2\beta q^2 \rho\|\Phi_2 - \Phi_1\|_{2 \rightarrow 2}\right) \\
& = 2q\rho(1 + 2q\beta\rho)\|\Phi_2 - \Phi_1\|_{2 \rightarrow 2}.
\end{aligned}$$

Overall, we obtain

$$\|\sigma(T_1(f_{\Phi_1}^L(Y))) - \sigma(T_2(f_{\Phi_2}^L(Y)))\|_F \leq \Sigma_L \|\Phi_2 - \Phi_1\|_{2 \rightarrow 2}, \quad (41)$$

where  $\Sigma_L = 2q\rho\sqrt{\beta}\left(K_L + \|A\|_{2 \rightarrow 2}\|Y\|_F q\sqrt{\beta} \sum_{k=0}^{L-1} G^k\right)$ .  $\square$

### 3.4 Chaining the Rademacher complexity

We apply the results of Sections 3.2 and 3.3 and estimate the covering numbers of an equivalent to (18) set, namely,

$$\begin{aligned}
\mathbf{M} & := \{(h(y_1)|h(y_2)|\dots|h(y_s)) \in \mathbb{R}^{n \times s} : h \in \mathbf{H}^L\} \\
& = \{\sigma(T(f_{\Phi}^L(Y))) \in \mathbb{R}^{n \times s} : \Phi \in \mathcal{F}_\beta\}.
\end{aligned} \quad (42)$$

The columns of each  $M \in \mathbf{M}$  constitute the reconstructions produced by  $h \in \mathbf{H}^L$  when applied to each  $y_i$ ,  $i = 1, 2, \dots, s$ . Since both  $\mathbf{M}$  and  $\mathbf{H}^L$  are parameterized by  $\Phi$ , we rewrite (28) as follows:

$$\mathcal{R}_S(\mathbf{H}) = \mathbb{E} \sup_{h \in \mathbf{H}^L} \sum_{i=1}^s \sum_{k=1}^n \epsilon_{ik} h_k(x_i) = \mathbb{E} \sup_{M \in \mathbf{M}} \frac{1}{s} \sum_{i=1}^s \sum_{k=1}^n \epsilon_{ik} M_{ik}. \quad (43)$$

The latter has subgaussian increments, so we employ Dudley's inequality [29, Theorem 8.23] to upper bound it in terms of the covering numbers of  $\mathbf{M}$ . A key quantity

appearing in Dudley's inequality is the radius of  $\mathbf{M}$ , that is,

$$\begin{aligned}\Delta(\mathbf{M}) &= \sup_{h \in \mathbf{H}^L} \sqrt{\mathbb{E} \left( \sum_{i=1}^s \sum_{k=1}^n \epsilon_{ik} h_k(y_i) \right)^2} \leq \sup_{h \in \mathbf{H}^L} \sqrt{\mathbb{E} \sum_{i=1}^s \sum_{k=1}^n \epsilon_{ik} (h_k(y_i))^2} \\ &\leq \sup_{h \in \mathbf{H}^L} \sqrt{\sum_{i=1}^s \|h(y_i)\|_2^2} \stackrel{(30)}{\leq} \sqrt{s} B_{\text{out}}.\end{aligned}\quad (44)$$

We combine (28), (43), (44) and apply Dudley's inequality to obtain

$$\mathcal{R}_S(l \circ \mathbf{H}^L) \leq \frac{16(B_{\text{in}} + B_{\text{out}})}{s} \int_0^{\frac{\sqrt{s} B_{\text{out}}}{2}} \sqrt{\log \mathcal{N}(\mathbf{M}, \|\cdot\|_F, \varepsilon)} d\varepsilon. \quad (45)$$

Finally, we estimate the quantity  $\mathcal{N}(\mathbf{M}, \|\cdot\|_F, \varepsilon)$ .

**Lemma 3.12.** *For  $0 < t < \infty$ , the covering numbers of the ball  $B_{\|\cdot\|_{2 \rightarrow 2}}^{N \times n}(t) = \{X \in \mathbb{R}^{N \times n} : \|X\|_{2 \rightarrow 2} \leq t\}$  satisfy the following for any  $\varepsilon > 0$ :*

$$\mathcal{N}(B_{\|\cdot\|_{2 \rightarrow 2}}^{N \times n}(t), \|\cdot\|_{2 \rightarrow 2}, \varepsilon) \leq \left(1 + \frac{2t}{\varepsilon}\right)^{Nn}. \quad (46)$$

*Proof.* For  $|\cdot|$  denoting the volume in  $\mathbb{R}^{N \times n}$ , we adapt a well-known result [54, Proposition 4.2.12], in order to connect covering numbers and  $|\cdot|$ :

$$\begin{aligned}\mathcal{N}(B_{\|\cdot\|_{2 \rightarrow 2}}^{N \times n}(t), \|\cdot\|_{2 \rightarrow 2}, \varepsilon) &\leq \frac{|B_{\|\cdot\|_{2 \rightarrow 2}}^{N \times n}(t) + (\frac{\varepsilon}{2})B_{\|\cdot\|_{2 \rightarrow 2}}^{N \times n}(1)|}{|(\frac{\varepsilon}{2})B_{\|\cdot\|_{2 \rightarrow 2}}^{N \times n}(1)|} = \frac{|(t + \frac{\varepsilon}{2})B_{\|\cdot\|_{2 \rightarrow 2}}^{N \times n}(1)|}{|(\frac{\varepsilon}{2})B_{\|\cdot\|_{2 \rightarrow 2}}^{N \times n}(1)|} \\ &\leq \left(1 + \frac{2t}{\varepsilon}\right)^{Nn}. \quad \square\end{aligned}$$

**Proposition 3.13.** *For the covering numbers of  $\mathbf{M}$  it holds:*

$$\mathcal{N}(\mathbf{M}, \|\cdot\|_F, \varepsilon) \leq \left(1 + \frac{2\sqrt{\beta}\Sigma_L}{\varepsilon}\right)^{Nn}. \quad (47)$$

*Proof.* By Definition 3.2 and Remark 3.3 we have  $\mathcal{F}_\beta \subset B_{\|\cdot\|_{2 \rightarrow 2}}^{N \times n}(\sqrt{\beta})$ . Then, the application of Lemma 3.12 implies for  $\mathcal{F}_\beta$  that

$$\mathcal{N}(\mathcal{F}_\beta, \|\cdot\|_{2 \rightarrow 2}, \varepsilon) \leq \left(1 + \frac{2\sqrt{\beta}}{\varepsilon}\right)^{Nn}. \quad (48)$$

Therefore, the covering numbers of  $\mathbf{M}$  are bounded as follows:

$$\begin{aligned}\mathcal{N}(\mathbf{M}, \|\cdot\|_F, \varepsilon) &\leq \mathcal{N}(\Sigma_L \mathcal{F}_\beta, \|\cdot\|_{2 \rightarrow 2}, \varepsilon) = \mathcal{N}(\mathcal{F}_\beta, \|\cdot\|_{2 \rightarrow 2}, \varepsilon/\Sigma_L) \\ &\leq \left(1 + \frac{2\sqrt{\beta}\Sigma_L}{\varepsilon}\right)^{Nn},\end{aligned}\quad (49)$$

which is the desired estimate.  $\square$

### 3.5 Generalization error bounds

We combine the results of Section 3.4 with Theorem 3.5, to deliver generalization error bounds for ADMM-DAD.

**Theorem 3.14.** *Let  $\mathbf{H}^L$  be the hypothesis class defined in (18). With probability at least  $1 - \delta$ , for all  $h \in \mathbf{H}^L$ , the generalization error is bounded as*

$$\begin{aligned} \mathcal{L}(h) &\leq \hat{\mathcal{L}}_{train}(h) + 8(B_{in} + B_{out})B_{out}\sqrt{\frac{Nn}{s}}\sqrt{\log\left(e\left(1 + \frac{2\sqrt{\beta}\Sigma_L}{\sqrt{s}B_{out}}\right)\right)} \\ &\quad + 4(B_{in} + B_{out})^2\sqrt{\frac{2\log(4/\delta)}{s}}, \end{aligned} \quad (50)$$

with  $\Sigma_L$  defined as in Corollary 3.11.

*Proof.* We apply Proposition 3.13 in (45) to get

$$\begin{aligned} \mathcal{R}_S(l \circ \mathbf{H}^L) &\leq \frac{16(B_{in} + B_{out})}{s} \int_0^{\frac{\sqrt{s}B_{out}}{2}} \sqrt{\log \mathcal{N}(\mathbf{M}, \|\cdot\|_F, \varepsilon)} d\varepsilon \\ &\leq \frac{16(B_{in} + B_{out})}{s} \int_0^{\frac{\sqrt{s}B_{out}}{2}} \sqrt{Nn \log\left(1 + \frac{2\sqrt{\beta}\Sigma_L}{\varepsilon}\right)} d\varepsilon \\ &\leq 8(B_{in} + B_{out})B_{out}\sqrt{\frac{Nn}{s}}\sqrt{\log\left(e\left(1 + \frac{4\sqrt{\beta}\Sigma_L}{\sqrt{s}B_{out}}\right)\right)}, \end{aligned} \quad (51)$$

where in the last step we used the following inequality:

$$\int_0^a \sqrt{\log\left(1 + \frac{b}{t}\right)} dt \leq a\sqrt{\log(e(1 + b/a))}, \quad a, b > 0.$$

We substitute the estimate (51) in Theorem 3.5 and the proof follows.  $\square$

**Theorem 3.15.** *Let  $\mathbf{H}^L$  be the hypothesis class defined in (18). Assume there exist pair-samples  $\{(x_i, y_i)\}_{i=1}^s \stackrel{i.i.d.}{\sim} \mathcal{D}^s$ , with  $y_i = Ax_i + e$ ,  $\|e\|_2 \leq \varepsilon$ , for some  $\varepsilon > 0$ . Let us further assume that it holds  $\|y_i\|_2 \leq B_{in}$  almost surely with  $B_{in} = B_{out}$  in (15). Then with probability at least  $1 - \delta$ , for all  $h \in \mathbf{H}^L$ , the generalization error is bounded as*

$$\begin{aligned} \mathcal{L}(h) &\leq \hat{\mathcal{L}}_{train}(h) + 16B_{out}^2 \left( \sqrt{\frac{Nn}{s}} \sqrt{\log\left(e\left(1 + \frac{2\sqrt{\beta}\Sigma_L}{\sqrt{s}B_{out}}\right)\right)} \right. \\ &\quad \left. + \sqrt{\frac{2\log(4/\delta)}{s}} \right), \end{aligned} \quad (52)$$

with  $\Sigma_L$  defined as in Corollary 3.11.

Notice that  $L$  enters at most exponentially in the definition of  $K_L$  (37) – and thus  $\Sigma_L$  (39). If we treat all terms in (52) as constants, except for  $L$ ,  $N$ ,  $s$ , then the previous Theorem tells us that the generalization error of ADMM-DAD roughly scales like  $\sqrt{NL/s}$ .

## 4 Experiments

We train and test ADMM-DAD on a synthetic dataset of random vectors, drawn from the normal distribution (70000 training and 10000 test examples) and the MNIST dataset [41], containing 60000 training and 10000 test  $28 \times 28$  image examples. For the MNIST dataset, we take the vectorized form of the images. We examine ADMM-DAD for alternating number of layers  $L$  and redundancy ratios  $N/n$ . For the measurement process, we select an appropriately normalized Gaussian matrix  $A \in \mathbb{R}^{m \times n}$ , with  $m/n = 25\%$  CS ratio. We also add zero-mean Gaussian noise  $e$ , with standard deviation  $\text{std} = 10^{-4}$  to the measurements, so that  $y = Ax + e$ . We perform (He) normal initialization [55] for  $W \in \mathbb{R}^{N \times n}$ . We implement all models in PyTorch [56] and train them using the *Adam* algorithm [57], with batch size 128. For all experiments, we report the *test MSE*:

$$\mathcal{L}_{test} = \frac{1}{d} \sum_{i=1}^d \|h(\tilde{y}_i) - \tilde{x}_i\|_2^2, \quad (53)$$

where  $\mathbf{D} = \{(\tilde{y}_i, \tilde{x}_i)\}_{i=1}^d$  is a set of  $d$  test data, that are not used during training, and the *empirical generalization error* (EGE)

$$\mathcal{L}_{gen} = |\mathcal{L}_{test} - \mathcal{L}_{train}|, \quad (54)$$

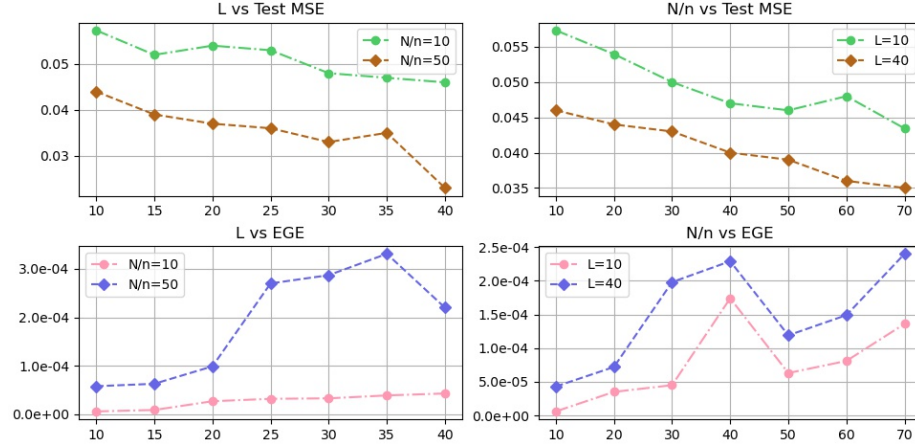
where  $\mathcal{L}_{train}$  is defined in (20). Since (53) approximates the true loss, we use (54) – which can be explicitly computed – to approximate (22). We train all models, on all datasets, employing early stopping [58] with respect to (54). We repeat all the experiments at least 10 times and average the results over the runs. We also compare ADMM-DAD to a recent variant of ISTA-net [20]. Both DUNs learn corresponding decoders for CS, but ISTA-net promotes synthesis sparsity, by learning an orthogonal sparsifying transform; ADMM-DAD, in contrast, promotes analysis sparsity by means of the learnable redundant analysis operator. Therefore, the structure of ISTA-net makes it a nice candidate for comparison with ADMM-DAD, in order to showcase how the reconstructive and generalization ability of DUNs are affected, when employing a redundant sparsifier instead of an orthogonal one. For ISTA-net, we set the best hyper-parameters proposed by the original authors.

### 4.1 Experimental results & discussion

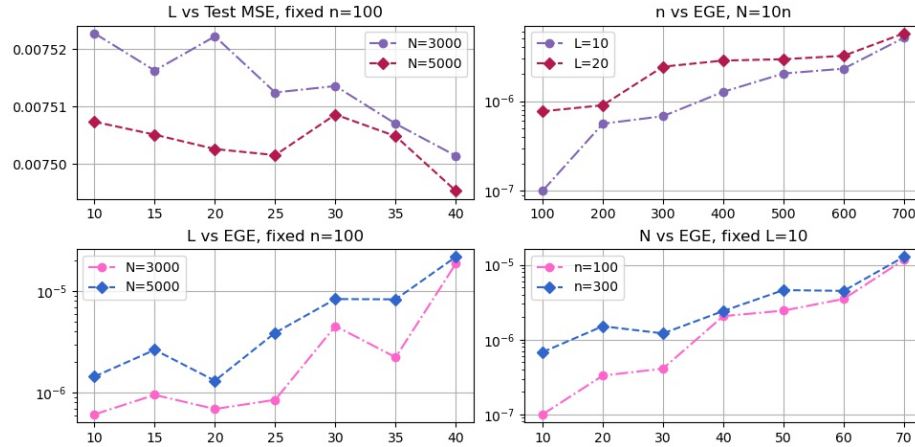
We evaluate the quality of our theoretical results with the following experimental scenarios.

#### 4.1.1 Varying $N$ , $L$ on real-world image data

We examine the performance of ADMM-DAD on MNIST dataset, with varying number of layers  $L$  and redundancy  $N$  of the learnable sparsifier. We gather the results in Figure 1a, which illustrates that the test MSE achieved by each instance of ADMM-DAD drops, as  $L$  and  $N$  increase. The decays seem reasonable, if examined from a model-based point of view. Specifically, when an iterative algorithm solves the generalized LASSO problem (5), it is expected that the reconstruction quality and performance of the solver will benefit from the (high) redundancy offered by the involved analysis operators [32], especially as the number of iterations/layers increases. On the other hand, the EGE of ADMM-DAD increases as both  $L$  and  $N/n$  increase. This behaviour



(a) Test MSEs and EGEs for MNIST



(b) Test MSEs and EGEs for synthetic data

Figure 1: Performance plots of ADMM-DAD on (a) MNIST and (b) synthetic datasets, for varying  $L$ ,  $N$  (and  $n$ ).

confirms the theory we developed in Section 3.5, since the EGE seems to scale like  $\sqrt{NL}$ .

		Test MSE					
Dataset		Synthetic			MNIST		
Decoder	Layers	$L = 10$	$L = 20$	$L = 30$	$L = 10$	$L = 20$	$L = 30$
ADMM-DAD (Ours)		<b>0.007725</b>	<b>0.007600</b>	<b>0.007586</b>	<b>0.046391</b>	<b>0.040282</b>	<b>0.032001</b>
ISTA-net [20]		0.007959	0.007774	0.007710	0.070645	0.068006	0.066325

		Generalization Error					
Dataset		Synthetic			MNIST		
Decoder	Layers	$L = 10$	$L = 20$	$L = 30$	$L = 10$	$L = 20$	$L = 30$
ADMM-DAD (Ours)		<b><math>0.22 \cdot 10^{-6}</math></b>	<b><math>1.04 \cdot 10^{-6}</math></b>	<b><math>1.65 \cdot 10^{-6}</math></b>	<b><math>0.63 \cdot 10^{-4}</math></b>	<b><math>0.40 \cdot 10^{-4}</math></b>	<b><math>1.21 \cdot 10^{-4}</math></b>
ISTA-net [20]		$4.48 \cdot 10^{-6}$	$2.64 \cdot 10^{-6}$	$9.44 \cdot 10^{-6}$	$22.51 \cdot 10^{-4}$	$50.45 \cdot 10^{-4}$	$76.16 \cdot 10^{-4}$

Table 1: Test MSEs and empirical generalization errors for 10-, 20- and 30-layer decoders, with fixed 25% CS ratio and redundancy ratio  $N/n = 50$ . Bold letters indicate the best performance between the two decoders.

#### 4.1.2 Varying $n$ , $N$ , $L$ on synthetic data

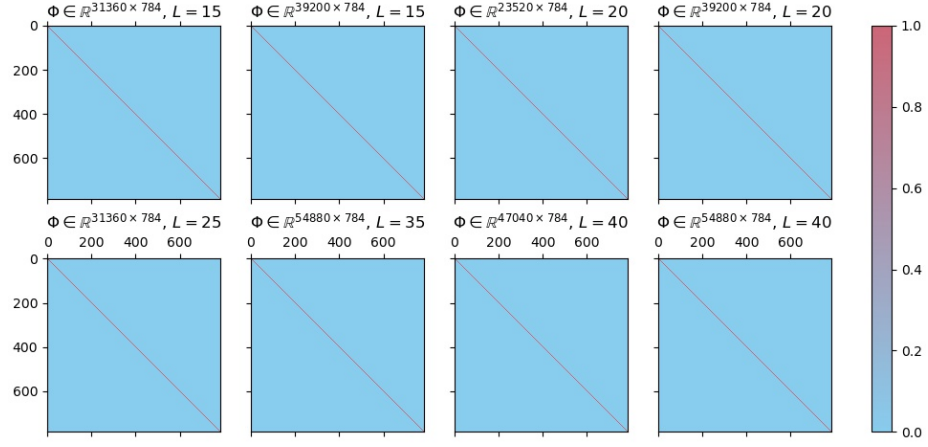
We test ADMM-DAD on a synthetic dataset, with varying  $L$ ,  $N$  and ambient dimension  $n$ . We report the results in Figure 1b, which illustrates the reconstruction error decreasing as  $L$  increases. Regarding the generalization error, we observe in Figure 1b that the EGE appears to grow at the rate of  $\sqrt{nNL}$ , despite the fact that the theoretical generalization error bounds depend on other terms as well. The overall performance of ADMM-DAD again conforms with our theoretical results.

#### 4.1.3 Comparison to baseline

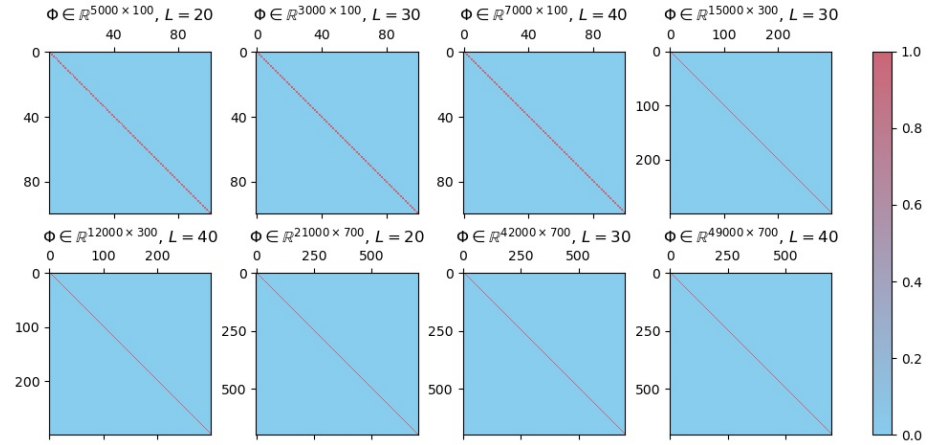
We examine how analysis and synthesis sparsity models affect the generalization ability of unfolding networks solving the CS problem. To that end, we compare the decoders of ADMM-DAD and ISTA-net, on the MNIST and the synthetic datasets, for varying

$(N, L)$	$\rho \ S^{-1}\ _{2 \rightarrow 2} \ A\ _{2 \rightarrow 2}$	$(n, N, L)$	$\rho \ S^{-1}\ _{2 \rightarrow 2} \ A\ _{2 \rightarrow 2}$
(23520, 10)	0.0003	(100, 1000, 10)	0.0031
(31360, 15)	0.0002	(100, 5000, 20)	0.0004
(39200, 15)	0.0002	(100, 3000, 30)	0.0007
(23520, 20)	0.0003	(100, 7000, 40)	0.0002
(39200, 20)	0.0002	(300, 21000, 10)	0.0003
(31360, 25)	0.0002	(300, 6000, 20)	0.0007
(7840, 30)	0.0021	(300, 15000, 30)	0.0002
(15680, 30)	0.0009	(300, 12000, 40)	0.0003
(54880, 35)	0.0001	(700, 21000, 20)	0.0002
(47040, 40)	0.0001	(700, 42000, 30)	0.0001
(54880, 40)	0.0001	(700, 49000, 40)	0.00008

Table 2: Examination of the values of  $\rho \|S^{-1}\|_{2 \rightarrow 2} \|A\|_{2 \rightarrow 2}$ , under different choices of  $L$ ,  $N$  (and  $n$ ), for the MNIST (left) and the synthetic (right) datasets.



(a) MNIST dataset



(b) Synthetic data

Figure 2: Visualization of  $S^{-1}S$  on (a) MNIST and (b) synthetic datasets, for varying  $L$ ,  $N$  (and  $n$ ) of the associated learnable  $\Phi$ .



number of layers. For the synthetic dataset, we fix the ambient dimension to  $n = 300$ . For ADMM-DAD, we set  $N = 39200$  for the sparsifier acting on the MNIST dataset and  $N = 15000$  for the sparsifier acting on the synthetic data. Our results are collected in Table 1. As depicted in the latter, ADMM-DAD’s decoder outperforms ISTA-net’s decoder, consistently for both datasets, in terms of both reconstruction and generalization error. For the former, our experiments confirm the model-based results regarding the advantage of analysis sparsity over its synthesis counterpart (cf. Section 2.2). As for the generalization error: our results indicate that the redundancy of the learnable sparsifier acts beneficially for the generalization ability of ADMM-DAD, compared to the orthogonality of ISTA-net’s framework.

#### 4.1.4 A note on the invertibility of $S = \Phi^T \Phi$

We revisit the setups of Sections 4.1.1, 4.1.2 and implement exemplary instances of ADMM-DAD, in order to verify Assumptions 3.1 and 3.2. To that end, we examine the values of  $S^{-1}S$  and  $\rho\|S^{-1}\|_{2 \rightarrow 2}\|A\|_{2 \rightarrow 2}$ , for fixed  $\rho = 0.1$ ,  $\|A\|_{2 \rightarrow 2} \approx 2$  and with  $S$ -operator associated to each learned  $\Phi$ , and present the results in Figure 2 and Table 2, respectively. According to the latter, the values of  $\rho\|S^{-1}\|_{2 \rightarrow 2}\|A\|_{2 \rightarrow 2}$  are consistently less than 1, for different tuples of  $L$ ,  $N$  (and  $n$ ), which is in accordance to Assumption 3.2. We also provide in Figure 2 a visualization of the structure of  $S^{-1}S$ . As illustrated in the aforementioned figure, ADMM-DAD learns a redundant analysis operator  $\Phi$  with associated  $S$ -operator satisfying<sup>2</sup>  $S^{-1}S = I$ . This observation validates our intuition for imposing Assumption 3.1 in our framework, as well as constraining  $\Phi$  to lie in  $\mathcal{F}_\beta$  (see Section 3.1). Furthermore, we conjecture that the fact that ADMM-DAD learns an analysis operator associated to a frame could explain its increased performance, compared to the synthesis-based baseline; this assumption could serve as a potential line of future work. Note that we have also conducted experiments with a regularizer of the form  $\|S^{-1}S - I\|_F$ , in order to cover the small probability of learning a  $\Phi$  such that  $S$  is not invertible. Since ADMM-DAD with and without the regularizer yielded almost identical performance, we chose to proceed with minimizing the train MSE only. Overall, this set of example experiments showcases that the appearance of the term  $\Phi^T \Phi$  in the iterative scheme of ADMM-DAD, induces a frame property to the learnable redundant analysis operator  $\Phi$ .

## 5 Conclusion and Future Work

In this paper, we studied the generalization ability of a state-of-the-art ADMM-based unfolding network, namely ADMM-DAD. The latter jointly learns a decoder for Compressed Sensing (CS) and a sparsifying redundant analysis operator. To that end, we first exploited an inherent characteristic of ADMM to impose a meaningful structural constraint on ADMM-DAD’s learnable sparsifier; the latter parametrized ADMM-DAD’s hypothesis class. Our novelty relies on the fact that the proposed framework induces a frame property on the learnable sparsifying transform. Then, we employed chaining to estimate the Rademacher complexity of ADMM-DAD’s hypothesis class. With this estimate in hand, we delivered generalization error bounds for ADMM-DAD. To our knowledge, we are the first to study the generalization ability of an ADMM-based unfolding network, that solves the analysis-based CS problem. Finally,

<sup>2</sup>Due to Python’s round-off errors, we consider the identity matrix  $I$  to have ones on the main diagonal and non-diagonal entries of the order at most  $10^{-5}$

we conducted experiments validating our theory and compared ADMM-DAD to a state-of-the-art unfolding network for CS; the former outperformed the latter, consistently for all datasets. As a future line of work, we would like to include more experiments regarding the structure of ADMM-DAD, especially with respect to the afore-stated frame property. Additionally, it would be interesting to include numerical comparisons among ADMM-DAD and ADMM-based unfolding networks promoting synthesis sparsity in CS.

## Acknowledgements

V. Kouni acknowledges financial support for the implementation of this paper by Greece and the European Union (European Social Fund-ESF) through the Operational Program “Human Resources Development, Education and Lifelong Learning” in the context of the Act “Enhancing Human Resources Research Potential by undertaking a Doctoral Research” Sub-action 2: IKY Scholarship Program for PhD candidates in the Greek Universities.

## Conflict of Interest Statement

On behalf of all authors, the corresponding author states that there is no conflict of interest.

## References

- [1] R. Chartrand and W. Yin. “Iteratively reweighted algorithms for compressive sensing”. In: *Int. Conf. Acoust., Speech and Signal Process.* IEEE. 2008, pp. 3869–3872.
- [2] I. Daubechies, M. Defrise, and C. De Mol. “An iterative thresholding algorithm for linear inverse problems with a sparsity constraint”. In: *Commun. Pure and Appl. Math.* 57.11 (2004), pp. 1413–1457.
- [3] A. Beck and M. Teboulle. “A fast iterative shrinkage-thresholding algorithm for linear inverse problems”. In: *SIAM J. Imag. Sci.* 2.1 (2009), pp. 183–202.
- [4] S. Boyd, N. Parikh, and E. Chu. *Distributed optimization and statistical learning via the alternating direction method of multipliers*. Now Publishers Inc, 2011.
- [5] S. Xu, S. Zeng, and J. Romberg. “Fast Compressive Sensing Recovery Using Generative Models with Structured Latent Variables”. In: *Int. Conf. Acoust., Speech and Sig. Process.* IEEE. 2019, pp. 2967–2971.
- [6] Z. Liu and J. Scarlett. “Information-theoretic lower bounds for compressive sensing with generative models”. In: *IEEE J. Selected Areas Inf. Theory* 1.1 (2020), pp. 292–303.

- [7] M. Shen et al. “TransCS: A Transformer-Based Hybrid Architecture for Image Compressed Sensing”. In: *IEEE Trans. Image Process.* 31 (2022), pp. 6991–7005.
- [8] J. R. Hershey, J. Le Roux, and F. Weninger. “Deep unfolding: Model-based inspiration of novel deep architectures”. In: *arXiv preprint arXiv:1409.2574* (2014).
- [9] V. Monga, Y. Li, and Y. C Eldar. “Algorithm unrolling: Interpretable, efficient deep learning for signal and image processing”. In: *IEEE Signal Process. Mag.* 38.2 (2021), pp. 18–44.
- [10] J. Scarlett et al. “Theoretical perspectives on deep learning methods in inverse problems”. In: *arXiv preprint arXiv:2206.14373* (2022).
- [11] W. An et al. “A Numerical DEs Perspective on Unfolded Linearized ADMM Networks for Inverse Problems”. In: *Proc. of the 30th ACM Int. Conf. Multimedia.* 2022, pp. 5065–5073.
- [12] M. Zhou et al. “Memory-augmented deep unfolding network for guided image super-resolution”. In: *Int. J. Comput. Vis.* 131.1 (2023), pp. 215–242.
- [13] J. Zhang et al. “Deep Unfolding With Weighted  $l_2$  Minimization for Compressive Sensing”. In: *IEEE Internet of Things J.* 8.4 (2020), pp. 3027–3041.
- [14] Q. Hu et al. “Iterative algorithm induced deep-unfolding neural networks: Precoding design for multiuser MIMO systems”. In: *IEEE Trans. Wirel. Commun.* 20.2 (2020), pp. 1394–1410.
- [15] S. Wisdom et al. “Building recurrent networks by unfolding iterative thresholding for sequential sparse recovery”. In: *Int. Conf. Acoust., Speech and Signal Process.* IEEE. 2017, pp. 4346–4350.
- [16] C. Mou, Q. Wang, and J. Zhang. “Deep Generalized Unfolding Networks for Image Restoration”. In: *Proc. Conf. Comput. Vision and Pattern Recogn.* IEEE. 2022, pp. 17399–17410.
- [17] Y. Yang, P. Xiao, and N. Deligiannis. “Underwater localization with binary measurements: From compressed sensing to deep unfolding”. In: *Digital Signal Process.* (2022), p. 103867.
- [18] C. Ma et al. “Deep Unfolding for Compressed Sensing with Denoiser”. In: *Int. Conf. Multimedia and Expo.* IEEE. 2022, pp. 01–06.
- [19] J. Sun et al. “Compressive Sensing via Unfolded  $l_0$ -constrained Convolutional Sparse Coding”. In: *Data Compress. Conf.* IEEE. 2021, pp. 183–192.
- [20] A. Behboodi, H. Rauhut, and E. Schnoor. “Compressive sensing and neural networks from a statistical learning perspective”. In: *Compressed Sensing in Information Processing.* Springer, 2022, pp. 247–277.

- [21] J. Zhang and B. Ghanem. “ISTA-Net: Interpretable optimization-inspired deep network for image compressive sensing”. In: *Proc. Comput. Vis. and Pattern Recognit.* IEEE. 2018, pp. 1828–1837.
- [22] J. Sun, H. Li, and Z. Xu. “Deep ADMM-Net for compressive sensing MRI”. In: *Advances Neural Inf. Process. Syst.* 29 (2016).
- [23] J. M. Ramirez, J. I. Martinez-Torre, and H. Arguello. “LADMM-Net: an unrolled deep network for spectral image fusion from compressive data”. In: *Signal Process.* 189 (2021), p. 108239.
- [24] V. Kouni et al. “ADMM-DAD Net: a Deep Unfolding Network for Analysis Compressed Sensing”. In: *Int. Conf. Acoust., Speech and Signal Process.* IEEE. 2022, pp. 1506–1510.
- [25] Jiawei Ma et al. “Deep tensor admm-net for snapshot compressive imaging”. In: *Proc. IEEE/CVF Int. Conf. Comput. Vis.* 2019, pp. 10223–10232.
- [26] H. Zayyani, M. Korki, and F. Marvasti. “Dictionary learning for blind one bit compressed sensing”. In: *IEEE Signal Process. Lett.* 23.2 (2015), pp. 187–191.
- [27] Y. Shen et al. “Image reconstruction algorithm from compressed sensing measurements by dictionary learning”. In: *Neurocomputing* 151 (2015), pp. 1153–1162.
- [28] Z. Li, H. Huang, and S. Misra. “Compressed sensing via dictionary learning and approximate message passing for multimedia Internet of Things”. In: *IEEE Internet of Things J.* 4.2 (2016), pp. 505–512.
- [29] S. Foucart and H. Rauhut. “An invitation to compressive sensing”. In: *A mathematical introduction to compressive sensing*. Springer, 2013, pp. 1–39.
- [30] E. J. Candes et al. “Compressed sensing with coherent and redundant dictionaries”. In: *Appl. and Comput. Harmon. Anal.* 31.1 (2011), pp. 59–73.
- [31] H. Cherkaoui et al. “Analysis vs synthesis-based regularization for combined compressed sensing and parallel MRI reconstruction at 7 tesla”. In: *Eur. Signal Process. Conf.* IEEE. 2018, pp. 36–40.
- [32] M. Genzel, G. Kutyniok, and M. März. “ $l_1$ -Analysis minimization and generalized (co-) sparsity: When does recovery succeed?” In: *Appl. and Comput. Harmon. Anal.* 52 (2021), pp. 82–140.
- [33] S. Shalev-Shwartz and S. Ben-David. *Understanding machine learning: From theory to algorithms*. Cambridge university press, 2014.
- [34] M. Mohri, A. Rostamizadeh, and A. Talwalkar. *Foundations of machine learning*. MIT press, 2018.
- [35] Y. Cao and Q. Gu. “Generalization bounds of stochastic gradient descent for wide and deep neural networks”. In: *Advances Neural Inf. Process. Syst.* 32 (2019).

- [36] H. Wang et al. “An information-theoretic view of generalization via Wasserstein distance”. In: *Int. Symp. Inf. Theory (ISIT)*. IEEE. 2019, pp. 577–581.
- [37] S. Arora et al. “Stronger generalization bounds for deep nets via a compression approach”. In: *Int. Conf. Mach. Learn.* PMLR. 2018, pp. 254–263.
- [38] P. L. Bartlett, D. J. Foster, and M. J. Telgarsky. “Spectrally-normalized margin bounds for neural networks”. In: *Advances Neur. Inf. Process. Syst.* 30 (2017).
- [39] Huynh Van L., B. Joukovsky, and N. Deligiannis. “Interpretable Deep Recurrent Neural Networks via Unfolding Reweighted  $\ell_1 - \ell_1$  Minimization: Architecture Design and Generalization Analysis”. In: *arXiv preprint arXiv:2003.08334* (2020).
- [40] B. Joukovsky et al. “Generalization error bounds for deep unfolding RNNs”. In: *Uncertain. Artif. Intell.* PMLR. 2021, pp. 1515–1524.
- [41] Y. LeCun et al. “Gradient-based learning applied to document recognition”. In: *Proc. IEEE* 86.11 (1998), pp. 2278–2324.
- [42] Ben Adcock, Anders C Hansen, and Bogdan Roman. “A note on compressed sensing of structured sparse wavelet coefficients from subsampled Fourier measurements”. In: *IEEE Signal Process. Lett.* 23.5 (2016), pp. 732–736.
- [43] K. Gregor and Y. LeCun. “Learning fast approximations of sparse coding”. In: *Proc. 27th Int. Conf. Mach. Learn.* 2010, pp. 399–406.
- [44] Yunyi Li, Xiefeng Cheng, and Guan Gui. “Co-robust-ADMM-net: Joint ADMM framework and DNN for robust sparse composite regularization”. In: *IEEE Access* 6 (2018), pp. 47943–47952.
- [45] Maryia Kabanava, Holger Rauhut, and Hui Zhang. “Robust analysis  $l_1$ -recovery from Gaussian measurements and total variation minimization”. In: *Eur. J. Appl. Math.* 26.6 (2015), pp. 917–929.
- [46] V. Kouni and H. Rauhut. “Spark Deficient Gabor Frame Provides a Novel Analysis Operator for Compressed Sensing”. In: *Int. Conf. Neural Inf. Process.* Springer. 2021, pp. 700–708.
- [47] S. Nam et al. “The cospase analysis model and algorithms”. In: *Appl. and Comput. Harmon. Anal.* 34.1 (2013), pp. 30–56.
- [48] Ole Christensen. *An introduction to frames and Riesz bases*. Vol. 7. Boston: Birkhäuser, 2003.
- [49] Peter G Casazza, Gitta Kutyniok, and Friedrich Philipp. “Introduction to finite frame theory”. In: *Finite frames: theory and applications* (2013), pp. 1–53.
- [50] Y. Zhu. “An augmented ADMM algorithm with application to the generalized lasso problem”. In: *J. of Comput. and Graphical Statist.* 26.1 (2017), pp. 195–204.

- [51] M. Kabanava and H. Rauhut. “Analysis  $l_1$ -recovery with frames and gaussian measurements”. In: *Acta Appl. Math.* 140.1 (2015), pp. 173–195.
- [52] E. J. Candes et al. “Compressed sensing with coherent and redundant dictionaries”. In: *Appl. and Comput. Harmon. Anal.* 31.1 (2011), pp. 59–73.
- [53] A. Maurer. “A vector-contraction inequality for rademacher complexities”. In: *Int. Conf. Algorithmic Learn. Theory*. Springer. 2016, pp. 3–17.
- [54] R. Vershynin. *High-dimensional probability: An introduction with applications in data science*. Vol. 47. Cambridge university press, 2018.
- [55] Kaiming He et al. “Delving deep into rectifiers: Surpassing human-level performance on imagenet classification”. In: *Proc. Int. Conf. Comput. Vis.* IEEE. 2015, pp. 1026–1034.
- [56] N. Ketkar. “Introduction to pytorch”. In: *Deep learning with python*. Springer, 2017, pp. 195–208.
- [57] D. P. Kingma and J. Ba. “Adam: A method for stochastic optimization”. In: *arXiv preprint arXiv:1412.6980* (2014).
- [58] L. Prechelt. “Early stopping-but when?” In: *Neural Networks: Tricks of the trade*. Springer, 1998, pp. 55–69.